

CRAB WAIST INTERACTION REGION FOR FCC- ee (TLEP) *

A. Bogomyagkov[†], E. Levichev, P. Piminov,
BINP, Novosibirsk 630090, Russia

Abstract

Design study of the accelerator that would fit 80-100 km tunnel called Future Circular Colliders (FCC) includes high-luminosity e^+e^- collider (FCC- ee aka (TLEP)) with center-of-mass energy from 90 to 350 GeV to study Higgs boson properties and perform precise measurements at the electroweak scale [1–3]. Crab waist interaction region provides collisions with luminosity higher than $2 \times 10^{36} \text{ cm}^{-2} \text{ sec}^{-1}$ at beam energy of 45 GeV. The small values of the beta functions at the interaction point and distant final focus lenses are the reasons for high nonlinear chromaticity limiting energy acceptance of the whole ring. The present paper presents estimations of nonlinear effects and describes practical solutions implemented in the design of the interaction region for correction of linear and nonlinear chromaticity of beta functions, and of betatron tune advances, of second and third order geometrical aberrations from the strong sextupoles pairs. The given design embraces realistic design of final focus quadrupoles, satisfies geometrical constraints of the tunnel layout.

INTRODUCTION

One of the limiting factors of high energy e^+e^- collider (FCC- ee aka (TLEP)) is beamstrahlung [4, 5], which limits the beam life time. Consideration of this effect by different authors gave several sets of parameters to achieve high luminosity and feasible beam lifetime. The first one is based on head-on collisions [6], the second is relying on crab waist collision scheme [7, 8] with crossing angle $2\theta = 30$ mrad. Both sets implement the same values of beta functions at the interaction point (IP): $\beta_x^* = 0.5$ m, $\beta_y^* = 0.001$ m and require energy acceptance of the ring more than $\pm 2\%$ to provide feasible beam life time. Advantages of the crab waist set are higher luminosity (7.5 times at 45 GeV) and crossing angle that provides natural separation of the bunches. The list of parameters relevant to present work is given in Table 1.

Lattice of the interaction region (IR) should satisfy several requirements:

1. Since successor to FCC- ee is proton accelerator, the IR tunnel should be as straight as possible;
2. Small values of IP beta functions produce large chromaticity, which should be compensated as locally as possible in order to minimize excitation of nonlinear chromaticity;

Table 1: Relevant Parameters for Crab Waist IR [7]

	Z	W	H	tt
Energy [GeV]	45	80	120	175
Perimeter [km]	100			
Crossing angle [mrad]	30			
Particles per bunch [10^{11}]	1	4	4.7	4
Number of bunches	29791	739	127	33
Energy spread [10^{-3}]	1.1	2.1	2.4	2.6
Emittance hor. [nm]	0.14	0.44	1	2.1
Emittance ver. [pm]	1	2	2	4.3
β_x^*/β_y^* [m]	0.5 / 0.001			
Luminosity / IP [$10^{34} \text{ cm}^{-2} \text{ s}^{-1}$]	212	36	9	1.3
Energy loss / turn [GeV]	0.03	0.3	1.7	7.7

3. Synchrotron radiation power loss should be significantly smaller than in the arcs;
4. Synchrotron radiation at high energy will produce flux of high energy gamma quanta, therefore the lattice should minimize detector background;
5. Small beta functions at IP enhance effects of nonlinear dynamics, decreasing dynamic aperture and energy acceptance of the ring, therefore the lattice should be optimized to provide large dynamic aperture and energy acceptance.

ESTIMATIONS

The following estimations are performed for vertical plain and marked with subindex y . Assuming that action of the first final focus (FF) quadrupole Q0 changes the sign of α function the quadrupole strength could be estimated as $K_1 L = -2/L^*$, where L^* is distance from the interaction point (IP). Chromaticity of beta function is best described by Montague functions [9]

$$b = \frac{1}{\beta} \frac{\partial \beta}{\partial \delta}, \quad (1)$$

$$a = \frac{\partial \alpha}{\partial \delta} - \frac{\alpha}{\beta} \frac{\partial \beta}{\partial \delta}, \quad (2)$$

* Work is supported by the Ministry of Education and Science of the Russian Federation

[†] A.V.Bogomyagkov@inp.nsk.su

where δ is relative energy deviation. Montague functions satisfy evolution equations

$$\frac{\partial b_y}{\partial s} = -\frac{2a_y}{\beta_y}, \quad (3)$$

$$\frac{\partial a_y}{\partial s} = (K_1 - K_2\eta_0)\beta_y + \frac{2b_y}{\beta_y}, \quad (4)$$

where K_1 and K_2 are quadrupole and sextupole strengths respectively, η_0 is the first order horizontal dispersion. Assuming that $b = 0$ and $a = 0$ at IP, then after the first quadrupole $Q0$ a_y rises to

$$a_y(Q0) = K_1 L \beta(Q0) \approx -2 \frac{L^*}{\beta_y^*}. \quad (5)$$

Influence of the other quadrupoles is significantly smaller, therefore we will neglect it and Montague functions then oscillate at double betatron frequency exchanging values being $\pi/2$ in phase apart

$$b_y(\varphi_y) = -a_y(Q0) \sin(2(\varphi_y - \varphi_y(Q0))), \quad (6)$$

$$a_y(\varphi_y) = a_y(Q0) \cos(2(\varphi_y - \varphi_y(Q0))). \quad (7)$$

The first and second order phase advance φ chromaticities are given

$$\frac{\partial \varphi_y}{\partial \delta} = \frac{1}{2} \int_0^\pi \beta_y (K_1 - K_2 \eta_0) ds, \quad (8)$$

$$\begin{aligned} \frac{\partial^2 \varphi_y}{\partial \delta^2} &= -2 \frac{\partial \varphi_y}{\partial \delta} - \int_0^\pi \beta_y K_2 \eta_1 ds + \\ &+ \frac{1}{2} \int_0^\pi \beta_y b_y (K_1 - K_2 \eta_0) ds, \end{aligned} \quad (9)$$

where η_1 is the second order horizontal dispersion. The largest beta function is in the first quadrupole, therefore its contribution in the first order chromaticity is cardinal and gives $\partial\varphi/\partial\delta \approx -L^*/\beta_y^*$. So far the distance from IP to the edge of the first quadrupole $Q0$ was chosen 2 m, making the distance to the center of $Q0$ $L^* = 2 + 3.6/2 = 3.8$ m. Substituting numerical values in the formulas above we have

$$\frac{\partial \varphi_y}{\partial \delta}(Q0) = -3.8 \times 10^3, \quad (10)$$

$$a_y(Q0) = -7.6 \times 10^3. \quad (11)$$

using necessary values from the IR lattice we will estimate contributions from the different terms in (9). In the quadrupole at the proper phase ($\pi/4 + n\pi/2$ phase from $Q0$) b_y reaches maximum of $b_y \approx -7.6 \times 10^3$. If for example such quadrupole has the strength $K_1 L = 0.16 * 2 \text{ m}^{-1}$ and $\beta_y = 100$ m then quadrupole's contribution to second order chromaticity is $\partial^2\varphi/\partial\delta^2 \approx 1.2 \times 10^5$. The strongest sextupoles are exactly π in phase away from the FF quadrupoles, therefore the value of $b \approx 0$ making contribution to second order chromaticity rather small, the second order dispersion is $\eta_1 \approx 1$ and $K_2 \times L \approx -9.5 * 0.5 \text{ m}^{-2}$, then contribution to the

second order chromaticity is $\partial^2\varphi/\partial\delta^2 \approx 5 \times 10^2$. Hence, the primary source of second order chromaticity is quadrupoles with large beta function chromaticity. Therefore the main sextupoles designed to cancel beta function chromaticity should be as small as possible number of quadrupoles away from the FF quadrupoles, and L^* should be minimized. However minimum distance is limited by detector requirements from one side and by construction design of first quadrupole $Q0$ from the other.

To finish estimations we will answer the question what values of chromaticity are needed. For that reason we expand tune dependence $Q = \varphi/(2\pi)$ with respect to energy deviation

$$Q(\delta) = Q_0 + Q_0' \delta + Q_0'' \frac{\delta^2}{2} + Q_0''' \frac{\delta^3}{6} + \dots,$$

where “'''” denotes $d/d\delta$. Assuming that $Q_0' = 2$ and demanding that $0 \leq Q(\delta) - Q_0 \leq 0.5$ we can draw an area of possible Q_0'' and Q_0''' (Figure 1). Since interaction region will be connected with remaining arcs, which will have their own chromaticities we tried to minimize second order chromaticity in our lattice.

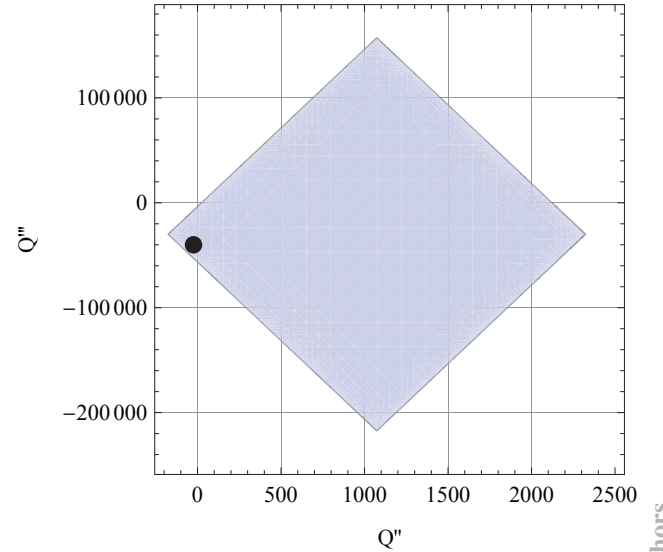


Figure 1: Area of Q_0'' and Q_0''' with $Q_0' = 2$ satisfying $0 \leq Q(\delta) - Q_0 \leq 0.5$ for $\delta \in [-0.02; 0.02]$. A dot represents the present lattice.

FINAL FOCUS QUADRUPOLES

Having the minimum distance the maximum reliably achievable gradient defines the quadrupole length. In the present study we demanded the quadrupole strength to be lower than 100 T/m, which is a very relaxed condition. We also chose distance from IP to the edge of first quadrupole to be 2 m which at the present moment looks like a good compromise between beam dynamics [10] and detector constraints. Particles trajectories from IP through the FF doublet are shown on Figure 2 together with lines at several angles representing detector blind spot and rectangles for

bare apertures of the quadrupoles. Quadrupole parameters length, gradient and radius of aperture at $E = 175$ Gev are presented in Table 2. The distance between bare apertures for the first quadrupoles is 3.5 cm, for the second pair the distance is 14.2 cm.

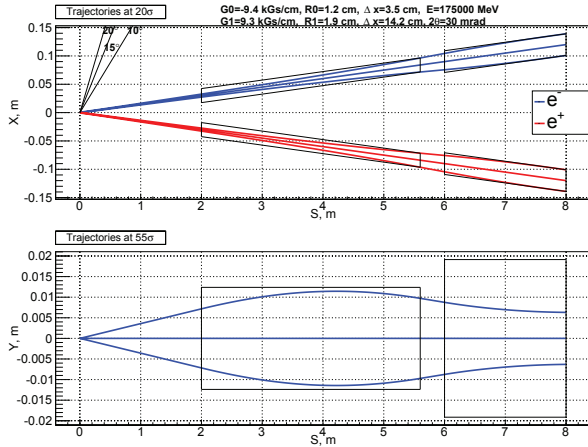


Figure 2: Trajectories of e^- and e^+ bunches from IP through FF quadrupoles. Several lines are drawn at 10° , 15° , 20° to represent blind solid angle of the detector. Black rectangles over trajectories depict bare quadrupole apertures.

Table 2: Parameters of FF Quadrupoles at 175 GeV

	L [m]	G [T/m]	R [m]
Q0	3.6	-94.5	0.012
Q1	2	93.3	0.019

LATTICE

The IR lattice should provide desired values of optical functions at IP and compensate geometrical and chromatic aberrations which define dynamic aperture (DA) and energy acceptance of the ring. The optics of IR consists of several blocks each having an intrinsic property of telescopic transformation: FFT — final focus telescope, CCSY and CCSX — chromaticity corrections section in horizontal (X) and vertical (Y) planes, CRAB — section that provides necessary phase advances and optical functions for crab waist sextupole [8]. The first dipole from IP is split in two, one closer to IP having a smaller field than the other. Redistribution of the field between the dipoles gives a useful knob to minimize synchrotron radiation background in the detector. The elements and optical functions are shown on Figure 3, optical blocks are also marked.

The overall geometry of the beam lines is shown on Figure 4. The divergence angle between beam lines is 8.8 mrad and will be intercepted by matching section to bring the beams into the arc.

Synchrotron radiation energy loss for the whole IR from one arc to the other is $2 \cdot 0.11 = 0.22$ GeV at beam energy

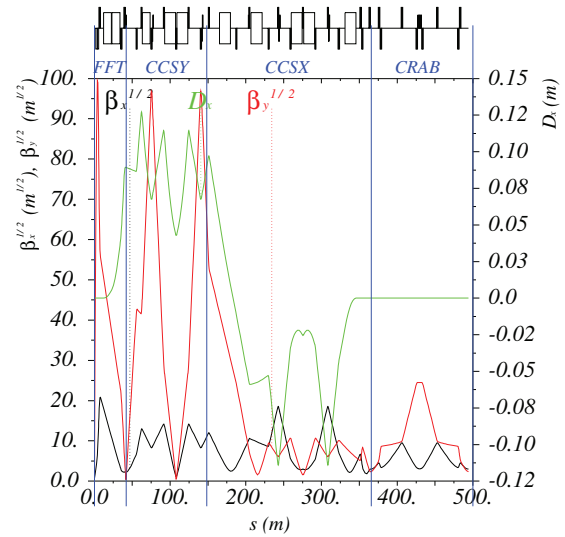


Figure 3: Optical functions of IR (version 6-12).

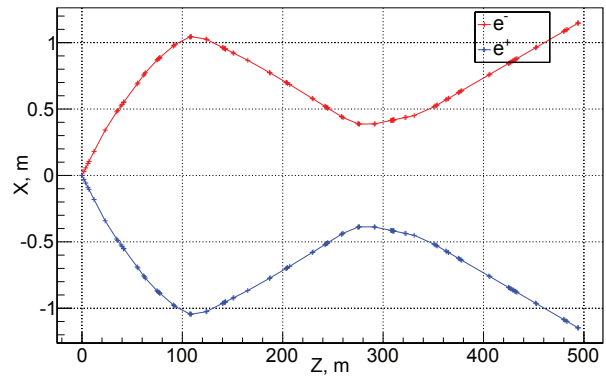


Figure 4: Layout of the electron and positron beam lines. Divergence of the beam lines is 8.8 mrad.

of 175 GeV. The relative power loss of four IPs with respect to the arcs is then $4 \cdot 0.22/7.7 = 0.11$.

CHROMATICITY

Chromatic functions $W = \sqrt{a^2 + b^2}$ are shown on Figure 5. Obtained phase advance chromaticities are given in Table 3. Shifting the sextupoles pairs in phase relative to corresponding FF quadrupole we minimized the second order chromaticities and satisfied our rough estimations. Introduction of two weak sextupoles in the places with small on-momentum beta function and large second order chromaticity of beta function allows to control third order chromaticity of phase advances and hope for no degradation of dynamic aperture. Results are shown in Table 3 and on Figures 6, 7, 8. Plots of beta function chromaticity at the end of IR are shown on Figures 9, 10, 11 for sextupoles in phase, sextupoles shifted in phase, sextupoles shifted in phase and two additional sextupoles. We need to note that results should be considered as demonstration of efficiency

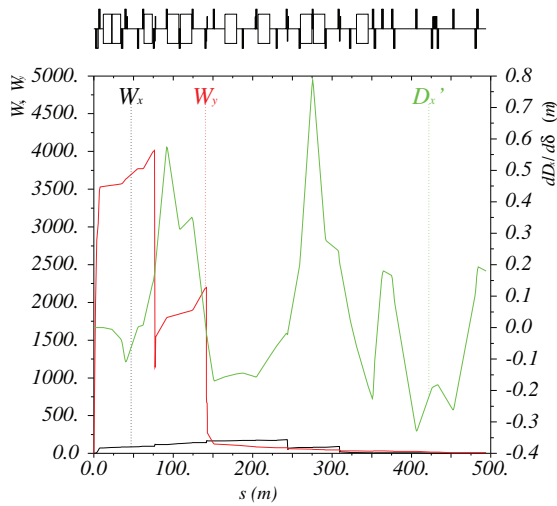


Figure 5: Chromatic (Montague) functions and nonlinear dispersion with sextupoles shifted in phase.

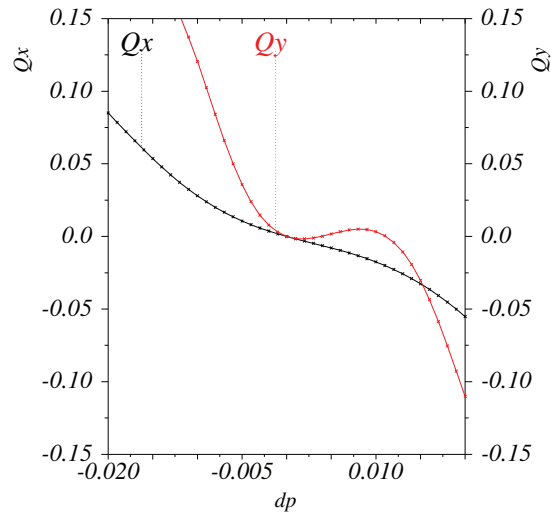


Figure 6: Phase advance variation with sextupoles in phase and no additional sextupoles.

of additional sextupoles, and they will have to be readjusted after the whole ring with realistic arcs is assembled.

Table 3: Chromaticity of Phase Advances from IP to the End of IR

	Sextupoles in phase	Sextupoles shifted	Sextupoles additional
Q_x		4	
Q'_x	-1.71	-1.62	-1.27
Q''_x	110	-48	-144
Q'''_x	$-3.6 \cdot 10^4$	$-3.4 \cdot 10^4$	$-2.9 \cdot 10^4$
Q''''_x	$-5.3 \cdot 10^5$	$7.4 \cdot 10^5$	$8.9 \cdot 10^5$
Q_y		3	
Q'_y	-2.15	-1.22	-1.51
Q''_y	$1.5 \cdot 10^3$	-38	-24
Q'''_y	$-3.1 \cdot 10^5$	$-3.1 \cdot 10^5$	$-4 \cdot 10^4$
Q''''_y	$-1 \cdot 10^6$	$5.8 \cdot 10^6$	$5.3 \cdot 10^6$

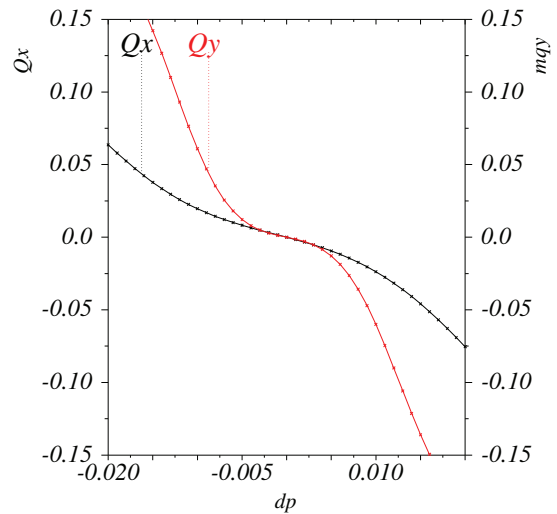


Figure 7: Phase advance variation with sextupoles shifted in phase and no additional sextupoles.

DYNAMIC APERTURE

We closed both shoulders of IR with linear map providing the fractional tunes $\nu_x = 0.54$ $\nu_y = 0.57$ in order to track particles through such a structure and study dynamic aperture. Optimization of sextupole's strengths gave the aperture of $R_x > 100 \cdot \sigma_x$ and $R_y > 200 \cdot \sigma_y$ (Figure 12) with no additional chromatic sextupoles. Each pair of main chromatic sextupoles has a pair of correcting sextupoles, whose strength is numerically adjusted in order to compensate for sextupole length effect [11].

CONCLUSION

We developed interaction region lattice with crossing angle for crab waist collision scheme. Geometrical layout, synchrotron radiation energy loss requirements are satisfied. Shifting sextupoles in phase with respect to final focus quadrupoles proves to be efficient method to minimize second order chromaticity of phase advances. Introduction of two additional sextupoles in the places with small values of beta functions gives useful knobs to control third order chromaticity. Chromatic aberrations are compensated and satisfy estimations. Estimation of dynamic aperture is done and found sufficient. Since, IP parameters are the same as in head-on collision scheme the lattice could be used without crab sextupole section in head-on collision scenario. The given lattice of interaction region will be readjusted after the close ring lattice with realistic arcs will be assembled,

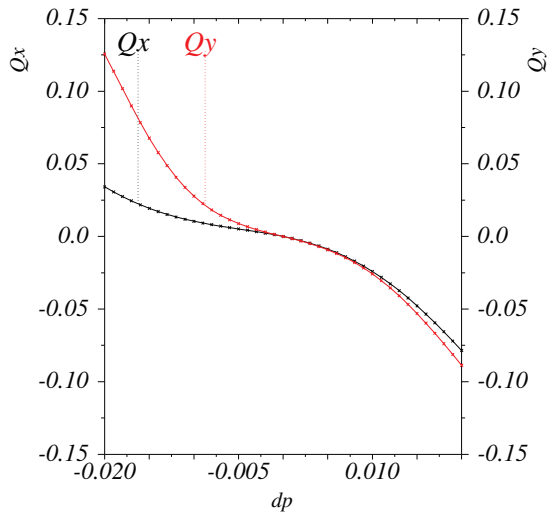


Figure 8: Phase advance variation with sextupoles shifted in phase and two additional sextupoles.

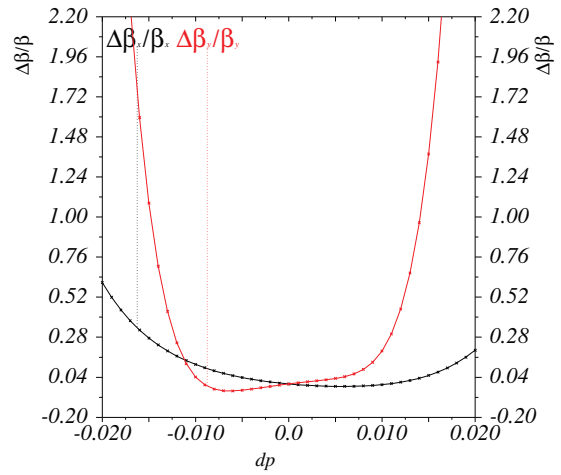


Figure 10: Chromaticity of the beta function at the end of IR with sextupoles shifted in phase and no additional sextupoles.

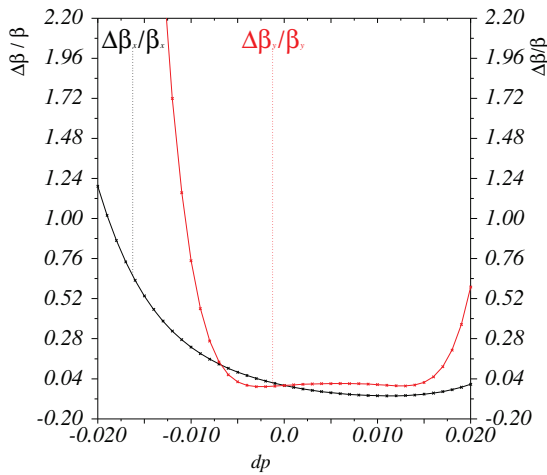


Figure 9: Chromaticity of the beta function at the end of IR with sextupoles in phase and no additional sextupoles.

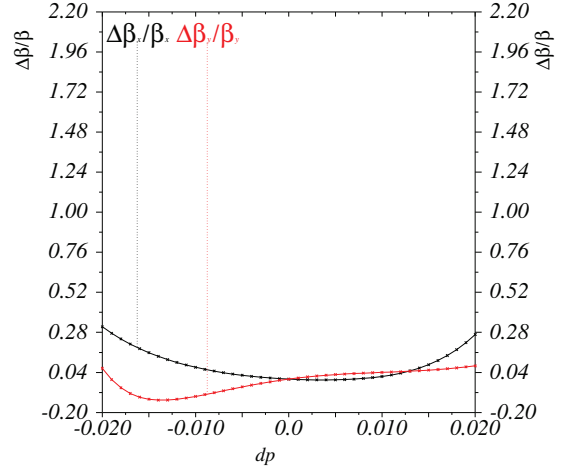


Figure 11: Chromaticity of the beta function at the end of IR with sextupoles shifted in phase and two additional sextupoles.

therefore it needs not be understood as fixed but rather work in progress.

There are several questions which we see important for immediate study.

1. Is it possible to build required final focus quadrupoles?
2. How longitudinal detector field will be compensated?
3. Is there a need to increase L^* ?
4. Do position and fields of the dipoles allow for synchrotron radiation shielding and detector background minimization?

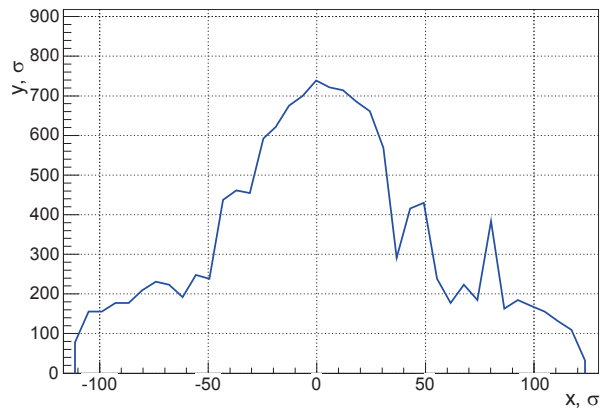


Figure 12: Dynamic aperture of the interaction region closed by the linear map $\sigma_x = 3.26 \cdot 10^{-5}$ m, $\sigma_y = 6.52 \cdot 10^{-8}$ m.

REFERENCES

- [1] M. Koratzinos et al., “TLEP: A HIGH-PERFORMANCE CIRCULAR e^+e^- COLLIDER TO STUDY THE HIGGS BOSON”, IPAC2013, Shanghai, China, TUPME040 (2013).
- [2] A. Blondel et al., “High luminosity e^+e^- storage ring colliders”, submitted to Phys. Rev. Special Topics: Accelerators and Beams; arXiv:1208.0504 [physics.acc-ph], (2012).
- [3] “The FCC-ee design study”, <http://tlep.web.cern.ch/>
- [4] J.E. Augustin et al., “Limitations on Performance of e^+e^- Storage Rings and Linear Colliding Beam Systems at High Energy”, ECONFC781015,009,(1978), <http://www.slac.stanford.edu/econf/C781015/pdf/009.pdf>
- [5] V.I. Telonov, “Restriction on the Energy and Luminosity of e^+e^- Storage Rings due to Beamstrahlung”, Phys. Rev. Lett.,110,114801 (2013), <http://link.aps.org/doi/10.1103/PhysRevLett.110.114801>
- [6] Headon parameters (2014), https://tlep.web.cern.ch/sites/tlep.web.cern.ch/files/LeptonColliderParameters_V1.0_0.pdf
- [7] A. Bogomyagkov et al., “Beam-beam effects investigation and parameters optimization for a circular e^+e^- collider at very high energies”, Phys. Rev. ST Accel. Beams. 17, 041004 (2014).
- [8] P. Raimondi, “Status of the SuperB effort”, 2nd Workshop on Super B factory, LNF-INFN, Frascati, March 2006.
- [9] B. W. Montague, “Linear Optics For Improved Chromaticity Correction,” CERN-LEP-NOTE-165.
- [10] A. Bogomyagkov et al., “Nonlinear properties of the FCC/TLEP final focus with respect to L^* ”, FCC-ee Accelerator VIDYO meeting No. 4 (2014), <http://indico.cern.ch/event/286658/>
- [11] A. Bogomyagkov, S. Glukhov, E. Levichev, P. Piminov, “Effect of the Sextupole Finite Length on Dynamic Aperture in the Collider Final Focus’, <http://arxiv.org/abs/0909.4872>, 2009